Journal of Geography and Cartography (2022) Volume 5 Issue 2
doi:10.24294/jgc.v5i2.1669

ORIGINAL RESEARCH ARTICLE

Noise mapping technology of high-speed railway based on GIS

Yanliang Li, Lanhua Liu, Zhiqiang Li*

Energy Saving & Environmental Protection & Occupational Safety and Health Research Institute, China Academy of Railway Sciences Corporation Limited, Beijing 100081, China. E-mail: qiangzhili123@163.com

ABSTRACT

In order to promote the application of noise map in high-speed railway noise management, the high-speed railway noise map drawing technology based on the combination of noise prediction model and geographic information system (GIS) is studied. Firstly, according to the distribution characteristics of noise sources and line structure characteristics of high-speed railway, the prediction model of multi equivalent sound sources and the calculation method of sound barrier insertion loss of high-speed railway are optimized; secondly, a three-dimensional geographic information model of a high-speed railway is built in GIS software, and the railway noise prediction technology based on the model is developed again; then, the noise of discrete nodes is calculated, and the continuous noise distribution map is drawn by spatial interpolation. The research results show that the comparison error between the noise map of a high-speed railway drawn by this technology and the measured results is less than 1 dB (A), which verifies the accuracy and practicality of the high-speed railway noise map, and can be used as a reference for the railway noise management department to formulate noise control countermeasures.

Keywords: High Speed Railway; Noise Prediction Model; Equivalent Sound Source; GIS; Noise Map

ARTICLE INFO

Received: 21 March 2022
Accepted: 10 May 2022
Available online: 16 May 2022

1. Introduction

Noise map is a kind of noise visualization technology that integrates computer, acoustics, geographic information and other disciplines, by transforming the abstract auditory perception of noise into intuitive and visual images, which significantly improves people's understanding of the degree and scope of noise impact, and has become an important technical means of environmental noise management at home and abroad. At present, noise maps at home and abroad are mostly used in regional urban noise research, but less in the railway industry. China has not yet formed a mature railway noise mapping technology[1].

There are three methods of noise mapping. The first is a direct drawing method combining monitoring data with geographic information system (GIS), which forms a noise distribution map by interpolating the monitoring data of a certain density. For example, the noise map of Madrid, Spain is drawn by interpolating the noise monitoring data from more than 4,000 monitoring points at 25 fixed monitoring stations and 14 mobile monitoring stations[2]. This method is suitable for drawing noise maps in a small range, the cost of noise monitoring is too high when it is widely used. The second method is to use noise prediction software to draw indirectly: first, using the mature noise prediction software (such as Cadna/A, Sound Plan or Lima, etc.) to calculate the noise distribution, and then publish the calculation results to GIS software to combine them

with geographic location information[3,4]. This method is the primary utilization and display of GIS, and does not have the spatial analysis function of deep mining geographic information in GIS. The third method is to deeply integrate noise prediction technology with GIS, extract spatial geographic information in GIS according to the needs of noise prediction parameters, realize the interactive application of noise prediction model and GIS, and draw a noise map that conforms to the actual geographical spatial characteristics[5].

Based on the third method of noise mapping, this paper takes a domestic high-speed railway as the research object, by optimizing the noise prediction model, builds the corresponding three-dimensional GIS model, studies the technical scheme of high-speed railway noise map, draws and publishes the first high-speed railway noise map in China.

2. Optimization of noise prediction model for high-speed railway

2.1 Three equivalent sound source model

Since 2010, the noise prediction of high-speed railway in China has mainly referred to the *Guiding Opinions on Noise Vibration Source Intensity Selection and Treatment Principles for Environmental Impact Assessment of Railway Construction Projects* (referred to as Railway Plan No. 44 document for short) issued by the former Ministry of railways. With the in-depth study of the noise characteristics of high-speed railway, experts and scholars in the industry believe that the noise prediction of high-speed railway should consider the sound generation mechanism and distribution characteristics of noise sources[6–8], and the method of three equivalent sound sources has gradually become the mainstream of domestic high-speed railway noise prediction. According to the identification results of high-speed railway noise sources in China, the noise sources can be divided into three parts: the lower areas, the car body area and the power collection system area [8-9], the lower part is dominated by wheel rail noise, which can be equivalent to a finite line sound source composed of incoherent dipole sources; the vehicle body area is dominated by the aerodynamic noise of the vehicle body, which can be equivalent to a finite line sound source composed of incoherent monopole sources; the area of the collecting system is dominated by the aerodynamic noise of the pantograph, which can be equivalent to the aerodynamic noise source of the dipole[10].

The division method of three equivalent sound sources is proposed from the perspective of sound source distribution, without considering the impact of track structure on noise sources.

2.2 Five equivalent sound source model and its verification

The cross-sectional diagram of typical line form of high-speed railway in China is shown in **Figure 1**.

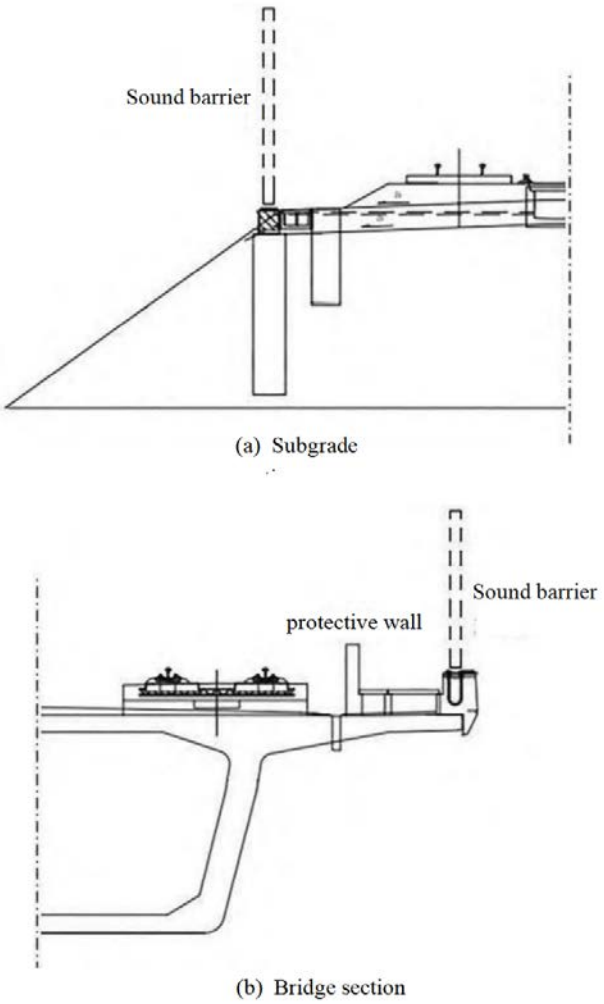

Figure 1. Cross section diagram of high-speed railway in China.

It can be seen from **Figure 1** that in the subgrade section, the outside of the track is relatively open, and the noise propagation of each equivalent

sound source is basically not affected; in the bridge section, the protective wall and bridge deck near the track will block the noise propagation in the lower area, causing large calculation errors. In addition, the typical height of the sound barrier of China's high-speed railway is 2.05 m above the rail surface, while the height of the EMU is about 4 m. Considering the whole vehicle body area as a single noise source in the sound barrier section will also lead to a large error in the calculation of the insertion loss of the sound barrier.

According to the structural differences of different line forms and the height characteristics of typical sound barriers, the distribution area of high-speed railway noise sources is further refined into five parts, and a more refined five equivalent sound source noise prediction model is constructed. The division of noise sources in each area is shown in **Figure 2.** See **Table 1** for the relationship between five equivalent sound sources and three equivalent sound sources.

According to the range division method of the three equivalent and fifth equivalent sound sources in **Figure 2** and **Table 1**, the noise source in the lower rail area and wheel area belongs to the lower area, and its noise propagation law conforms to formula (1); the noise sources of the two parts of the car body belong to the car body area, and the noise propagation law conforms to equation (2), and the noise propagation law of the collector system area conforms to equation (3). By superposition of the noise contribution of each equivalent sound source at the prediction point P through equation (4), the equivalent sound level L_{eq} of the train passing at point P can be obtained. The above formulas are

$$L_{Pl} = L_{Wl} + 10\lg\left(\frac{4l}{4d^2 + l^2} + \frac{1}{d}\arctan\frac{l}{2d}\right) - 8 \quad (1)$$

Where: L_{Pl} is the equivalent noise level of the contribution of the noise source in the under-rail area or wheel area to the prediction point P, dB(A); L_{Wl} is the sound power level of the noise source under the rail or in the wheel area, dB(A); d is the linear distance from the prediction point to the corresponding sound source, m; L is the length of EMU, M.

$$L_{Pf} = L_{Wf} + 10\lg\left(\frac{1}{d}\arctan\frac{l}{2d}\right) - 5 \quad (2)$$

Where: L_{Pf} is the equivalent noise level of the contribution of the noise source in the lower half or upper half of the vehicle body to the prediction point P, dB(A); L_{Wf} is the sound power level of the noise source in the lower or upper part of the vehicle body, dB(A).

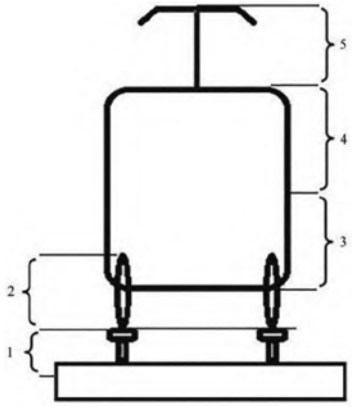

Figure 2. Diagram of five equivalent sound source division.

Table 1. Division of three equivalent sound sources and five equivalent sound sources

Three equivalent sound source area	Five equivalent sound source area	Longitudinal range	Vertical range	Equivalent height/m
Lower area	Under track area	Head to tail	Track slab–rail top	-0.10
	Wheel area	Head to tail	Rail top to wheel top	0.46
Vehicle body area	Lower part of vehicle body	Head to tail	From vehicle bottom to vehicle body	1.30
	Upper part of vehicle body	Head to tail	From the middle of the car body to the roof	2.80
Electricity collection system area	Electricity collection system area	3 m before and after the contact point of pantograph and catenary	Roof to catenary	5.20

$$L_{Pp} = L_{wp} - 5.4 + 10\lg\left[\left(\frac{1}{d}\arctan\frac{l-l_1}{d} + \frac{l-l_1}{d^2+(l-l_1)^2} + \frac{1}{d}\arctan\frac{l_1}{d} + \frac{l_1}{d^2+l_1^2}\right)\frac{1}{v}\right] \quad (3)$$

$$L_{eq} = 10\lg\left(10^{\frac{L_{P1}}{10}} + 10^{\frac{L_{P1}}{10}} + 10^{\frac{L_{Pp}}{10}}\right) \quad (4)$$

Where: L_{Pp} is the equivalent noise level of the contribution of the noise source in the collector area to the prediction point P, dB(A); L_{W_p} is the sound power level of the noise source in the collector system area, dB(A); l_1 is the distance between pantograph and train head; v is the running speed of EMU, km·h^{-1}.

In order to verify the accuracy advantage of the five equivalent sound source model over the three equivalent sound source model, measuring points of different heights are arranged at the bridge section of the studied high-speed railway at a distance of 25 m from the center line of the outer rail to monitor the equivalent sound level L_{eq} when the EMU passes the test section at a speed of 350 km·h^{-1} in 24 hours a day, and measure the maximum, minimum, mean and prediction results of the three equivalent sound source model as shown in **Figure 3**, **A** is a benchmark value. It can be seen from **Figure 3** that the predicted values of the three equivalent sound source model and the five equivalent sound source model at 3.5 m above the rail top are basically consistent with the measured mean values; as the height of the measuring point decreases, the impact of the protective wall and bridge structure on the noise in the lower area gradually increases. The difference between the predicted value of the three equivalent sound source model and the measured mean value can reach 1 dB(A), while the predicted value of the five equivalent sound source model is closer to the measured mean value, and the difference is less than 0.4 dB(A); when the height of the measuring point is further reduced and the noise source in the lower area of the bridge is blocked as a whole, the three equivalent sound source model is established. The difference between the predicted value of the five equivalent sound source model and the measured mean value shows a decreasing trend.

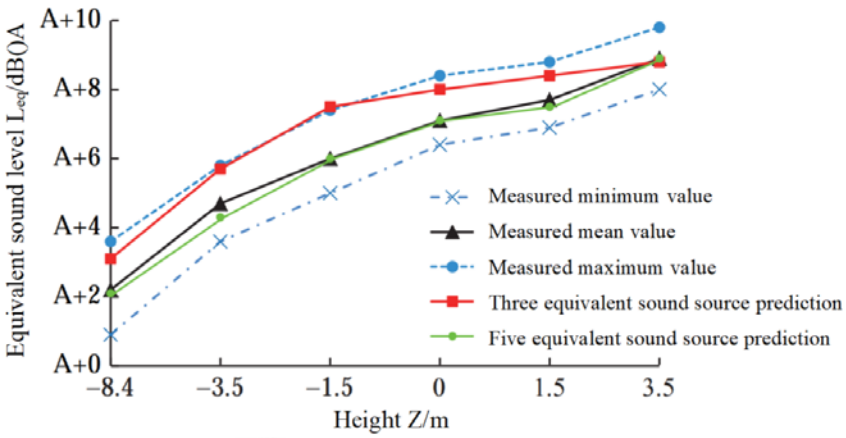

Figure 3. Measured and predicted equivalent sound levels at different heights 25m from the center line of the outer rail.

It can be seen that the five equivalent sound source model is a refinement of the three equivalent sound source model based on the specific line structure characteristics. Although the increase in the number of equivalent sound sources will increase the computational complexity, it can effectively reduce the impact of line structure differences on the prediction results and make the prediction results more accurate.

2.3 Correction of insertion loss at the end of sound barrier

There is a significant difference in the noise shielding effect of the sound barrier on the EMU driving to its end and middle position. In order to analyze the rationality and effectiveness of the design length of the sound barrier through the noise map, the influence of the additional length of the sound barrier on the noise reduction effect should be considered in the prediction algorithm of the noise map. Li and Liu proposed a formula for calculating

the insertion loss of sound barriers with different additional lengths[11].

$$R_P(a) = -10\lg\left[\frac{\frac{l}{2}+a}{l}10^{-\frac{R}{10}} + \frac{\frac{l}{2}-a}{l}\left(\frac{\sqrt{y^2+a^2}}{y}\right)^{-\frac{n}{10}}\right] \quad (5)$$

Where: a is the additional length of the sound barrier relative to the prediction point, m; $R_P(a)$ is the insertion loss of prediction point P when the additional length of sound barrier is a, dB(A); y is the straight-line distance from the prediction point to the track centerline, m; n is the constant of equivalent sound level attenuation with lg$y$ during the passage period of EMU; R is the insertion loss of the sound barrier to the prediction point P after all the emus drive into the sound barrier, dB(A).

When using equation (5) to calculate the insertion loss of the sound barrier at different positions at the end of the sound barrier, a, y, l can be obtained by predicting the relative position relationship between the point and the line and the type of EMU. In addition, the values of R and n need to be known. The R value can be obtained by comparing the calculation or measured results of the silent barrier section and the sound barrier section, and the n value can be obtained by using the trend line fitting method after predicting the noise at different distances.

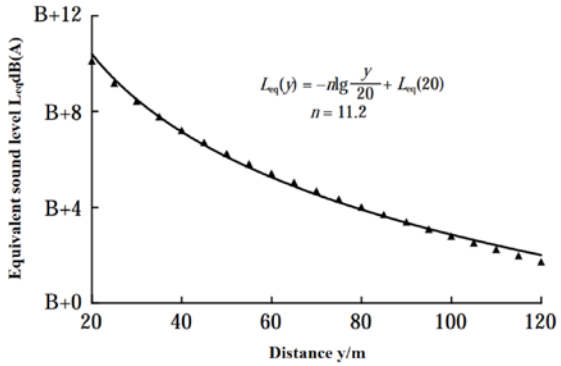

Figure 4. Noise variation with distance.

The variation law of bridge section noise with distance of the studied high-speed railway is analyzed and the results are shown in **Figure 4**. In the figure: B is a reference value. It can be seen from **Figure 4** that the value of n is about 11.2 according to the noise fitting result within the range of 20–120 m from the center line of the outer rail. Using the same method, the value of subgrade section n is about 10.8.

In the typical open line section of high-speed railway, the five equivalent sound source prediction model can be directly used to calculate the train passing equivalent sound level; in the sound barrier section, based on the five equivalent sound source noise prediction model, the prediction results need to be corrected by using the calculation method of the insertion loss of the sound barrier and the correction method of the insertion loss at the end of the sound barrier in Railway Plan No. 44 document; other environmental conditions that need to be corrected for noise shall be implemented in accordance with the corresponding provisions of Railway Plan No. 44 document. Five equivalent sound source noise prediction model, Railway Plan No. 44 document and the insertion loss correction method at the end of the sound barrier together constitute the theoretical model of noise prediction used in the high-speed railway noise map.

3. Noise map drawing based on GIS

According to the calculation parameters involved in the high-speed railway noise prediction model, the key geographic information required to draw the high-speed railway noise map mainly includes the relative position between the prediction point and the line, the terrain fluctuations, the building impact, the line form (bridge, subgrade) and the range and height of the section of the sound barrier installation, etc., so it is necessary to build a three-dimensional GIS model containing the above key information based on the above requirements.

3.1 3D GIS model construction

The satellite image map, elevation data (DEM), railway building vector factor data and railway rail center line factor are loaded on the GIS desktop. Take the elevation data as the elevation source to form undulating terrain, vertically stretch the building vector surface elements according to the building height attribute, and set the building elevation above the ground to form three-dimensional building body elements, so as to obtain the required three-dimensional basic geographic information model, as shown

in **Figure 5**.

Figure 5. 3D basic geographic information model.

Because the elevation data does not contain the line height information, the current basic geographic information model cannot extract the relative height of the line between the receiving point and its corresponding section. Information such as line form and sound barrier installation, so it is necessary to carry out a separate three-dimensional design for high-speed railway. To make the railway line contain both information about height, line form and sound barrier installation, a three-dimensional railway model needs to be built. The process is shown in **Figure 6**, which mainly includes the following steps.

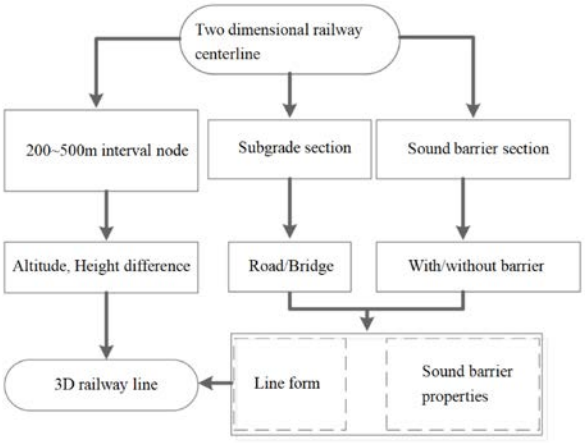

Figure 6. Construction process of 3D railway model.

Step 1: discretize the two-dimensional railway centerline into nodes along the line, and supplement the key nodes of the line fluctuation according to the railway profile.

Step 2: extract the elevation information in the node, add the elevation difference information, and use "elevation + elevation difference" to build the node height attribute.

Step 3: connect the nodes in order of height attributes to generate a 3D railway line.

Step 4: create the surface elements of subgrade section and sound barrier section, and intersect them with the two-dimensional railway centerline respectively to obtain the subgrade/bridge section, division of sections with/without sound barriers, and the corresponding height information of sound barriers shall be given to the sound barrier sections.

Step 5: the line form is analyzed through proximity analysis and connection analysis. Attributes such as sound barrier are assigned to the corresponding sections of the three-dimensional railway line according to the relative position relationship with the line.

Through the above operations, a 3D GIS model including 3D railway is constructed. For any position in the model, the corresponding geographic information parameters can be extracted through spatial analysis as the basic data for noise prediction and calculation.

3.2 Noise data generation and visualization

In order to establish a noise database containing ready to use geographic data information, the analysis area surface can be meshed, and the calculated noise value of the grid center point can be taken as the noise value in the whole grid surface, so as to realize the rapid construction of the noise database. However, the noise image obtained by this method is at the complex boundary (such as the contour of the building). At the boundary of the curve section), jagged shape will be produced, and mosaic phenomenon will be produced at the position where the noise changes significantly[5], which will have a great impact on the display effect of the noise. Therefore, through the interpolation analysis of the noise at discrete points to form a continuous noise cloud, we can get more detailed and continuous noise distribution data.

Create a noise map drawing buffer zone within a certain range on both sides of the high-speed railway centerline (taking the distance of 10–250 m from the railway centerline as an example), and

generate discrete noise analysis nodes in this area according to a certain grid density. On the one hand, the geographic information of each noise analysis node is extracted from the geographic database, and the analysis nodes are connected with the center line of the high-speed railway. Spatial analysis of terrain and buildings along the line to obtain noise propagation path parameters; on the other hand, the analysis nodes and the high-speed railway are analyzed for proximity and connection, and the line form and sound barrier type of the section are extracted to obtain the noise source and obstacle impact correction parameters. Input the parameters into the high-speed railway noise prediction model, calculate the equivalent sound level at each node of the EMU passing through the period, and use Crikin interpolation method to generate continuous noise grid data in the buffer zone, render colors according to the size of the noise value, and realize the visualization of the noise in the map. The equivalent sound level distribution map of emus passing through the period within 250 m on both sides of a high-speed railway generated by the above method is shown in **Figure 7**. Through the noise map, the noise impact on both sides of the high-speed railway can be observed intuitively.

In order to verify the accuracy of noise mapping results, in front of the building in a community on the side of the high-speed railway uplink studied. The noise of emus in the upward direction is tested and counted at multiple locations between buildings and behind buildings. The location of each measuring point is shown in **Figure 8** (the pop-up window is the calculation result of noise map at one measuring point). See **Table 2** for the comparison between the measured results and the noise map calculation results.

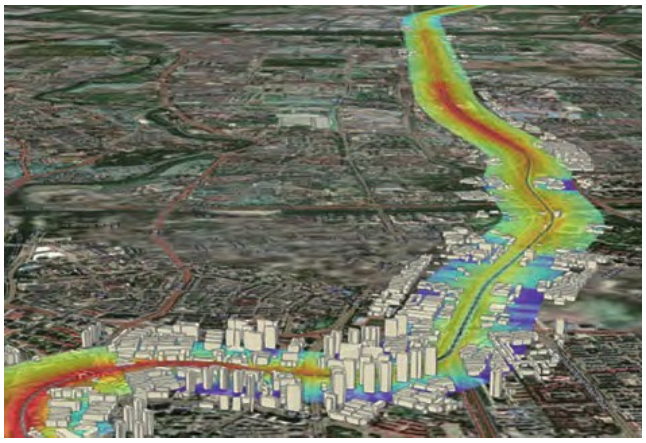

Figure 7. Noise map of a high-speed railway.

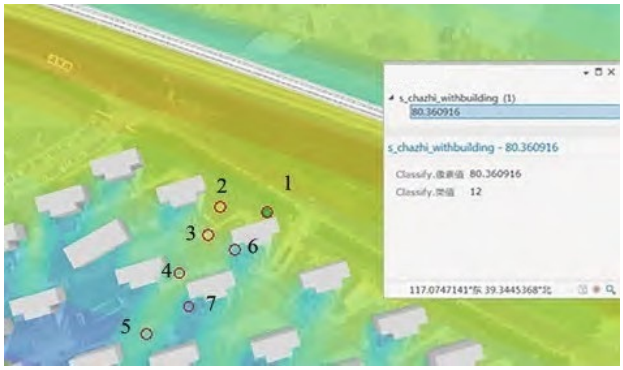

Figure 8. Location of noise map verification measuring points of a high-speed railway.

It can be seen from **Table 2** that the difference between the calculated value of the noise map at each measuring point and the measured mean value is 0.1–0.7 dB(A), indicating that the high-speed railway noise map drawn by this method has high accuracy and can meet the needs of practical application.

Table 2. Comparison between measured results and noise map calculation results dB(A)

Measuring point	Measured value			Map calculation value	Difference between the measured mean value and the calculated value of the map
	Minimum value	Maximum value	Mean value		
1	79.8	83.1	81.1	80.4	0.7
2	79.5	82.0	80.7	80.5	0.2
3	77.5	81.2	78.9	78.8	0.1
4	74.8	77.7	75.7	75.6	0.1
5	72.2	75.6	73.5	72.8	0.7
6	72.6	77.2	75.2	75.1	0.1
7	70.3	73.8	71.7	71.4	0.3

After the noise map of equivalent sound level of EMU passing period is formed, it can be further determined according to the traffic flow. Calculate the railway contribution noise map in any period of

time, such as the equivalent sound level per hour. The daytime equivalent sound level and night equivalent sound level are used to analyze the dynamic changes of railway contribution noise in different periods of time and the impact size and scope of railway noise in different sound function areas.

4. High speed railway noise map release

The above-mentioned high-speed railway noise map is drawn and displayed with the help of professional geographic information software, which users still need to use when accessing data, resulting in poor versatility of the noise map. In order to facilitate users to directly access the high-speed railway noise map results, it is necessary to publish and manage the relevant data.

The schematic diagram of high-speed railway noise map publishing scheme based on WebGIS is shown in **Figure 9**. Firstly, the processed geographic information data and noise data are released to the GIS Server by using the desktop GIS software, and the primary display application of relevant data is built on the server; secondly, common geographic information service functions such as geographic information annotation, retrieval and geographic ranging of GIS server are added, and server-side graphics scaling, roaming, data screening and statistical analysis tools are designed to enhance the practicability of noise map application; finally, the server-side application is shared to the network terminal, and users can use computers and handheld terminals to access the noise map data in the server through IE browser or other special browsing software.

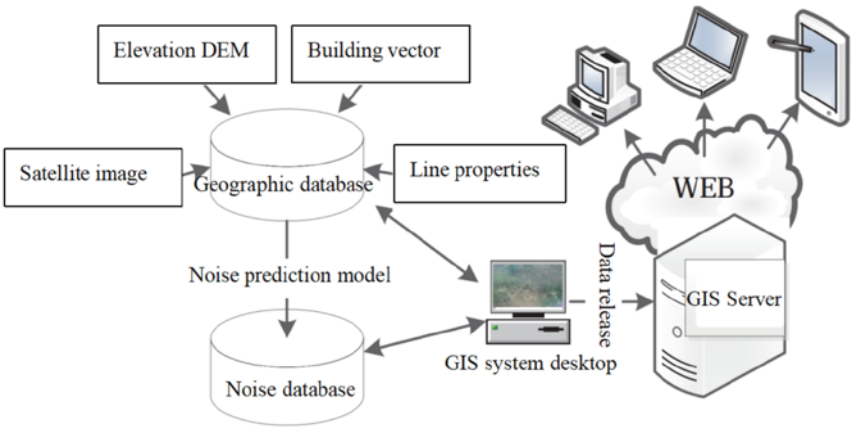

Figure 9. Schematic diagram of high-speed railway noise map publishing service scheme.

5. Conclusion

On the basis of optimizing the high-speed railway noise prediction model, this paper builds a three-dimensional geographic information model according to the parameter requirements of the high-speed railway noise prediction model, proposes a high-speed railway noise map technology integrating the high-speed railway noise prediction model and GIS model, successfully draws the first high-speed railway noise map in China, and studies the technical scheme of noise map publishing using Web-GIS. The comparison between the drawing results of the high-speed railway noise map and the field measured data shows that the error between the calculation results of the high-speed railway noise map based on GIS and the measured results is less than 1 dB(A) (between 0.1–0.7 dB(A)), which proves that the noise map technology has high accuracy and can be used as an important basis for the railway noise management department to formulate Noise Supervision and control countermeasures. The wide application of this technology in China’s high-speed railway network will effectively improve the noise management technology level of China's high-speed railway.

As an efficient and intuitive noise visualization technology means, noise map is one of the important development directions of noise management in the future. With the rapid growth of China's high-speed railway operating mileage and the new development trend of “high-speed railway entering the city”, the

high-speed railway noise map will become an important part of the urban regional noise map, and will play an important role in urban and railway planning, noise pollution prevention, smart high-speed rail, information high-speed rail, which is of great significance for promoting the digitalization, intelligence and modernization of China's high-speed railway environmental noise management.

References

1. Fan C, Wang T, Zhou B, *et al.* The development trend of noise map. Environmental Engineering 2016; 34(Supplement 1): 1095–1098.
2. Manvell D, Ballarin ML, Stapelfeldt H, *et al.* SADMAM combining measurements and calculations to map noise in Madrid. INTER-NOISE and NOISE-CON Congress and Conference Proceedings; 2004 Aug 22. Prague: Institute of Noise Control Engineering; 2004. p. 1998–2005.
3. Peng Y. Making and application of road traffic noise map of Luohu district of Shenzhen City. Environmental Monitoring and Forewarning 2014; 6(2): 42–44.
4. Xia D, Zhou Y, Zhu W. Study on application of noise mapping to noise environment management. Noise and Vibration Control 2013; 33(4): 162–166.
5. Cai M, Chen H, Ma X. 3D noise map based on GIS and OpenGL. Environmental Engineering 2015; 33(5): 111–113.
6. Su W, Pan X, Ye P. The study of acoustic computing model for the noise barrier of high-speed railway. China Railway Science 2013; 34(1): 126–130.
7. Ju L, Ge J, Guo Y. Model of high-speed railway noise prediction based on multi-source mode. Journal of Tongji University: Natural Science 2017; 45(1): 58–63.
8. Liu L, Sun J, Li Z, *et al.* A research on the calculation method of noise reduction effect of high-speed railway noise barriers based on 3 equivalent noise source model. Railway Transport and Economy 2018; 40(10): 81–87.
9. Li Y, Li Z, He C, *et al.* External noise source identification of Chinese high-speed EMU based on algorithm optimization. China Railway Science 2019; 40(1): 94–101.
10. Wu X. A study on the prediction methods of railway environmental noise. Railway Transport and Economy; 2018, 40(12): 98–103.
11. Li Z, Liu L. A new method for calculating the additional length of noise barrier on high-speed railway. Proceedings of 2020 Western China Acoustic Symposium. Shanghai: Technical Acoustics; 2020: 312–315.